International Journal of Electrical Engineering.
ISSN 0974-2158 Volume 5, Number 1 (2012), pp. 7-22

http://www.irphouse.com

# Transient Stability of Squirrel Cage Induction Generator in a Wind Farm using Static Synchronous Compensator and Supercapacitor

**[1]Vanitha V. and [2]Dr. Devarajan N.**

*[1]Assistant Professor, Department of Electrical and Electronics Engineering, Amrita Vishwa Vidyapeetham, Coimbatore, India*
*[2]Associate Professor, Department of Electrical and Electronics Engineering, Government College of Technology, Coimbatore, India*
*E-mail: v_vanitha@cb.amrita.edu*

**Abstract**

STATCOM is a static synchronous compensator operated as shunt connected static VAR compensator whose inductive or capacitive output current can be controlled independent of AC system voltage. It can rapidly supply dynamic VARs required during system disturbances and faults for voltage support. However, because of less energy density of DC link capacitor used in STATCOM, there is a large voltage dip in DC link voltage which limits the reactive power capability of STATCOM. Recent developments in the field of super capacitors have led to the achievement of high specific energy and high specific power devices which are suitable for energy storage in high power electronic applications. Super capacitor is very fast charging and discharging compared to traditional capacitors which is needed to restore the system quickly after the fault has been cleared so as to maintain system stability and to avoid tripping of SCIG coupled to wind turbine in wind farm. This chapter examines the use of STATCOM with Super Capacitor Energy Storage System to improve power quality of SCIG in the event of any unbalanced or balanced fault in the grid under different fault conditions. Analysis is done for different load conditions also.

**Keywords:** Supercapacitor, STATCOM Equivalent Series Resistance, Capacitance, Transient stability, fault

## Introduction

In the field of energy storage, two main parameters the energy density and the power density are fundamental for storage devices. The ideal storage device should propose both a high energy density, together with a high power density. This is unfortunately

not the case, and compromises have to be done. Considering the battery technologies, the energy density is high, but they have a poor power density. The opposite is the main characteristic of conventional capacitors, a limited power density with a high power density. New components, such as the supercapacitors, offer today an alternative to this dilemma. They are the compromise between batteries and conventional capacitors. Their main characteristic is to propose both a high energy density together with a high power density. This leads to new applications for energy storage, even if the energy density is still lower than that of the batteries.

Capacitors are broadly classified as electrostatic, electrolytic and electrochemical capacitors[2][5]. Electrostatic capacitors are typically made of two metal electrodes (parallel plates) separated by a dielectric. The dielectric is a non-conducting material (*e.g.,* air, plastic, paper, Mylar, etc.) that is inserted between the parallel plates of the metal electrode material. The strength of the dielectric material measured in volts per meter determines the operating voltage of the capacitor. The dielectric strength equals the maximum electric field that can exist in a dielectric without electrical breakdown. The dielectric increases the overall capacitance and the maximum operating voltage of the capacitor. The capacitance, measured in Farads, is defined as the ratio of total charge in coulombs in each electrode to the potential difference between the plates. The capacitance is also proportional to the surface area of the plates and inversely proportional to the distance between the plates multiplied by a permittivity constant. The stored energy of the capacitor in joules is proportional to the capacitance and voltage square across the plates. An electrolytic capacitor is similar in construction to an electrostatic capacitor but has a conductive electrolyte salt in direct contact with the metal electrodes. Aluminum electrolytic capacitors, for example, are made up of two aluminum conducting foils (one coated with an insulating oxide layer) and a paper spacer soaked in electrolyte. The oxide layer serves as the dielectric and is very thin, which results in higher capacitance per unit volume than electrostatic capacitors. Electrolytic capacitors have plus and minus polarity due to the oxide layer, which is held in place by the electric field established during charge. If the polarity is reverse-biased, the oxide layer dissolves in the electrolyte and can become shorted and, in extreme cases, the electrolyte can heat up and explode.

In general, Electrochemical Capacitors(ECs) also use electrolyte solutions but have even greater capacitance per unit volume due to their porous electrode structure compared to electrostatic and electrolytic capacitors. At the macroscopic level, the EC takes the equation $C = \varepsilon 0A/d$ to the extreme by having a very high electrode surface area ($A$) due to the porous electrodes and very small separation $d$ between the electronic and ionic charge at the electrode surface. Indeed, the surface area of the porous electrodes has been recorded to be as large as 1000 to 2000 $m^2/cm^3$. The high energy density of ECs is due to their greater capacitance per unit volume compared to conventional capacitors. ECs themselves are grouped into two major categories—symmetric and asymmetric. Symmetric ECs use the same electrode material (usually carbon) for both the positive and negative electrodes. Asymmetric ECs use two different materials for the positive and negative electrodes. Symmetric ECs get their electrostatic charge from the accumulation and separation of ions at the interface between the electrolyte and electrodes. Asymmetric ECs, in contrast, get their charge

from the reduction and oxidation (redox) reaction. Redox is the charge transfer of electrons that takes place at the electrode and electrolyte interface due to change in oxidation state. When an electric potential is applied to the current collectors, electrons accumulate on the negative electrode thus attracting the positively charged cations to accumulate on the electrode surface to balance the charge locally. Similarly, on the positive electrodes, the electron vacancies attract the negatively charged anions to settle on the electrode surface to balance the charge. This separation of ionic and electronic charge gave rise to the name 'double-layer' capacitors. Double-layer capacitance forms on each electrode in the presence of electric potential. The double-layer capacitance at the positive and negative electrodes adds in series to the total capacitance of the device. The amount of ion accumulation depends on the electric potential—the higher the electric potential, the higher the concentration of ions at the surface. Furthermore, with the presence of the electric potential, two layers are formed in the electrolyte near the electrode surface, the inner layer (also known as the Helmholtz layer) and the outer (or diffused) layer. The inner layer primarily consists of non conducting solvent molecules. The outer layer mainly consists of solvated ions (ions surrounded by solvent molecules) that are attracted to and held near the electrode through long-range electrostatic forces. The distance between the ions and the electrode particle is analogous to the parallel plate dielectric separation in conventional capacitor. The distance ($d$) can be only a few angstroms wide. The high surface area of the porous electrodes combined with a very small dielectric width or distance at the double-layer is the key to establishing high capacitance. The double-layer capacitance can range from 10 to 40 μF per $cm^2$. Thus, double-layer capacitors can range from a single Farad to thousands of Farads, unlike conventional capacitors which are rated in the nano- to micro-Farad range. The electrolyte remains conductive, with solvated ions held away from the electrode surface to allow for conduction between the double-layer capacitances at the positive and negative electrodes during charge and discharge. Over the years, ECs have acquired many names such as supercapacitor, ultracapacitor, Pseudocapacitor, Double layer capacitor etc. Symmetric ECs can use aqueous or organic electrolyte solutions. Aqueous electrolyte allows a maximum voltage of 1V per cell. If an organic electrolyte is used, the maximum allowable voltage per cell is 2.5V. A number of ultracapacitor cells are connected to form an Ultracapcitor module.

## Test Results of 100pp14 Supercapacitor

Fig 1 shows the test setup for charging and discharging 100PP14 supercapacitor available in Aartech Solonics Ltd., Bhopal. Super capacitor used in this paper is 100PP14, which is rated for 100V having an energy density of 14.2 kJ. It is an Electrochemical Double Layer Capacitor having bipolar symmetric carbon/carbon electrodes and an aqueous KOH electrolyte. It has internal balancing circuits. Its characteristics are high power cycling capacity of 300, 000 cycles, wide operating temperature of -45 degrees to +55 degrees, quick recharge of less than 10 seconds and free form fire and explosion hazards because of rugged construction. Equivalent circuit used for the conventional capacitor can also be applied to supercapacitors. First

order model of an supercapacitor is comprised of four ideal circuit elements, a capacitance C, Series resistor Rs, Parallel resistor Rp and series inductor L.Rs is called Equivalent Series Resistance(ESR), which contributes to energy loss during supercapacitor charging and discharging. Rp indicates energy loss due to capacitor self-discharge and is often referred to as leakage current resistance. Inductor L results primarily from the physical construction of capacitor and is usually small, which can be neglected. In the classical model of supercapacitor, the inductance L is neglected. These equivalent circuit parameters can be found by conducting charging and discharging experiments on the supercapacitor. It uses aqueous KOH (potassium hydroxide) electrolyte.The individual cells in the module are connected in series and parallel to get the desired voltage and capacitance. Equivalent circuit parameters of supercapacitor were obtained from charging and discharging tests.

**Figure 1:** Charging and Discharging set up of 100PP14

100PP14 supercapacitor is charged to the rated voltage of 100V from an AC source through an autotransformer. A filter capacitance of 470 microfarad and 250V is used to remove ripples in DC voltage output. Once it reaches the rated voltage, supercapacitor is discharged through a load resistance of 28.6 ohms, 250W. Fig 2 shows the charging and discharging characteristics of 100PP14. Table 1 and 2 show the results.

**Table 1:** Self discharge results of 100PP14.

| TIME(s) | VOLTAGE(V) |
|---|---|
| 0 | 100 |
| 240 | 96.9 |
| 600 | 95 |

**Table 2:** Charge and discharge results of 100PP14.

| Transient Voltage drop(V) | Current(A) | Time to discharge to half the rated voltage(s) | Load resistance (Ω) |
|---|---|---|---|
| 0.44 | 3.496 | 65 | 28.6 |

From the results, 100PP14 supercapacitor's equivalent circuit parameters are found to be:
$C_{CALC}$ = 3.278F
DC ESR = 0.125 Ω
DC EPR = 5398.166 Ω

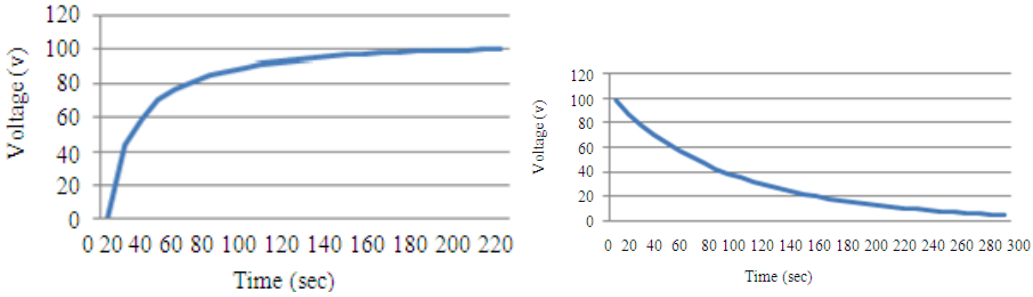


**Figure 2:** Charging and discharging characteristics of 100PP14.

## Static Synchronous Compensator (STATCOM)

During the last few decades, development of power electronics technology has helped to propose and implement Flexible AC Transmission Systems (FACTS) devices for overcoming power quality problems in power system[4]. The STATCOM has faster dynamic response than the SVC and usually there is no additional passive filter network needed for the STATCOM. Fig. 3 shows the single line diagram of STATCOM. STATCOM (Static Synchronous Compensator) is one of the most important FACTS devices based on the use of self commutated semiconductors. The STATCOM hardware is based on voltage source converters, a capacitor in its DC side and the converter controller[4]. It is connected to a power system through step up transformer.

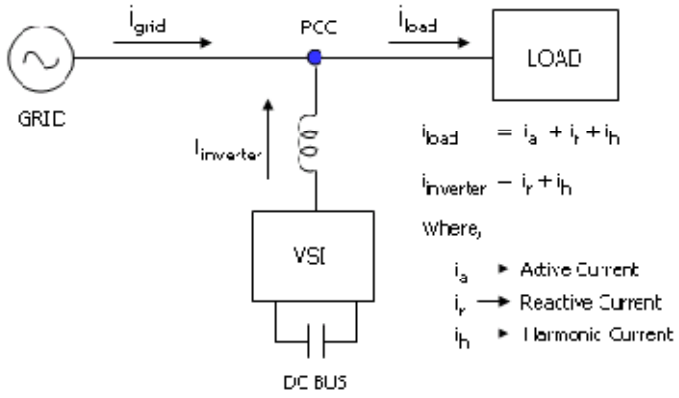


**Figure 3:** Single line diagram of STATCOM.

DC capacitor has direct influence on harmonics of output voltage generated by STATCOM and speed of response of controller. If capacitor is oversized, the controller's response will be fast but DC link voltage will have excessive ripples and consequently the output voltage will contain high levels of harmonic distortion. Moreover high transient overshoots will exist. On the other hand, an undersized capacitor will improve the shape of output voltage waveform and reduce the transient overshoots but at the expense of a slow controller response. Selection of shunt reactor has a large impact on the performance of STATCOM. Amplitude and phase angle of voltage drop across the reactor define the active and reactive power flows between STATCOM and AC system. This reactor will attenuate medium and higher order harmonics in STATCOM output voltage.

## Controllers of STATCOM

In STATCOM, the control strategy implemented is based on vector control principle[6]. The reactive current injected is controlled so as to obtain full rated grid voltage before, during and after the fault. The aim is to make the VSI continuously track and deliver the reactive currents demanded by the reactive load. It is based on the measurement of voltage at Point of Common Coupling(PCC).The voltage error signal is obtained by comparing the actual and reference voltage, which is fed to a PI controller. There needs to be another voltage controller to maintain a constant DC bus voltage. The STATCOM current is continuously compared with reference current received from two voltage controllers and error signal is fed into the Hysteresis comparator. Fig. 4 shows the block diagram of the vector control scheme for STATCOM.

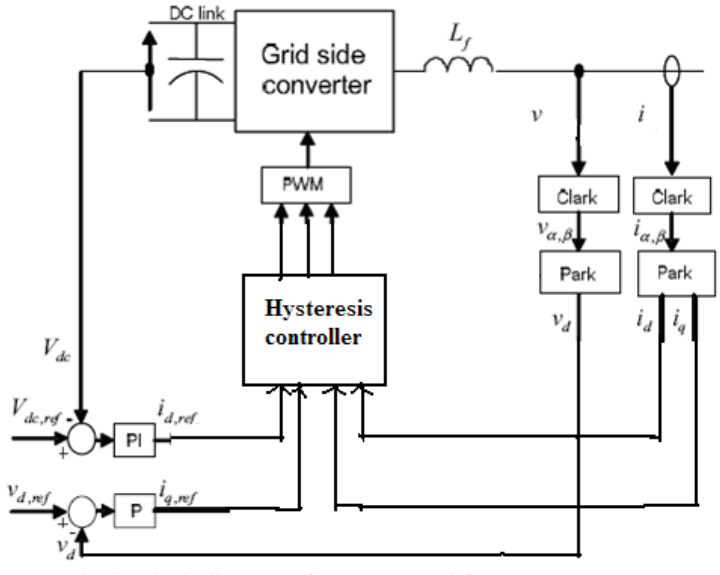


**Figure 4:** Block diagram of the Vector Control Scheme for STATCOM.

## Simulation Results of 250 kW SCIG Connected To 2000KVA Alternator

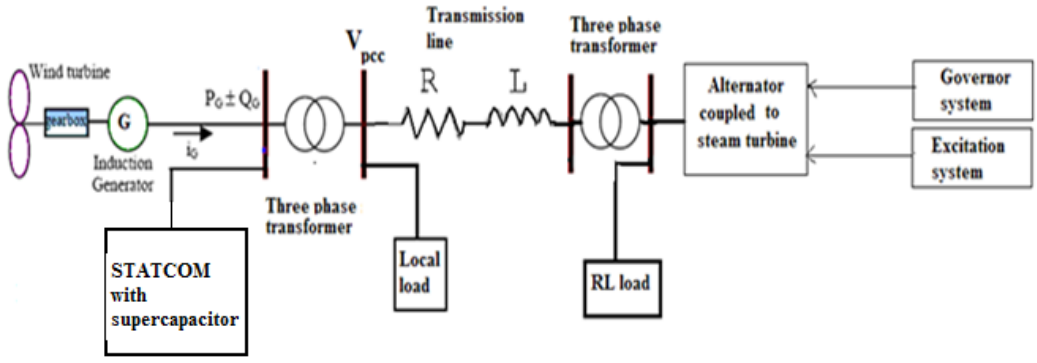


**Figure 5:** Schematic diagram of the system under study.

Fig 5 shows the schematic diagram of the system chosen for the study. Penetration level is defined as the ratio of the aggregate capacity of grid-connected WEGs to the aggregate capacity of conventional alternators on the grid. The load connected to the system is assumed to be of 0.9 power factor lagging. The penetration level of WEG is 12.5% as a steam turbine- alternator of 2000 kVA capacity is connected to the 250 kW SCIG coupled to a wind turbine. In transmission and distribution applications, supercapacitors have to be connected in series in order to withstand high voltage stress. The supercapacitor to be used here is connected in parallel with STATCOM DC link capacitor rated for 600V.So, six supercapacitors of 100PP14 can be connected in series so that the net capacitance value of the supercapacitor module is 0.55F and ESR is 0.75 ohms[3]. Hence the super capacitor is modeled with 0.55F capacitance, 750milli ohms ESR and a parallel resistance of 900 ohms. STATCOM with 250kVAR capacity is connected with supercapacitor at PCC. Equivalent model of six 100PP14 supercapacitors in series are connected in parallel with DC link capacitor of STATCOM in order to match the voltage of 600V[1]. The 250kW SCIG is connected to the grid via a transmission line X/R ratio 1.6.A local load of SCIG capacity is also connected at PCC.A fault is implemented at PCC and attention is focused on type and duration of faults.

Simulation of the system shown is carried out for different wind speeds ranging from the cut in speed of 5m/s to the rated wind speed of 15m/s considering rated output at higher wind speeds upto the cut out wind speed. The following performance indices of the system obtained as simulation results are tabulated in Table 3:

(i) ω, shaft speed of SCIG, (ii) P, real power generated by SCIG, (iii) Q, reactive power consumed by SCIG, (iv) Te, electromagnetic torque developed by SCIG, (v) Vpcc, voltage at the PCC, for different wind speeds, v.

Alternator speed settles at 1pu for all wind speeds. A 250kW SCIG draws 100kVAR reactive power when it is supplying full rated real power. A STATCOM of 250kVAR with the modified model of super capacitor is installed at PCC. The transient stability of SCIG under different fault conditions of various fault duration using STATCOM with supercapacitor compensation is studied. Performance with different penetration levels are also analyzed for each type of fault.

**Table 3:** Steady state values of different parameters at SCIG terminals for different wind speeds.

| Wind speed v(m/s) | SCIG speed (ω) in rad/sec | Real power generated P(kW) | Reactive power absorbed Q(kVAR) | Electromagnetic Torque Te(Nm) | Voltage at PCC (pu) |
|---|---|---|---|---|---|
| 8 | 157.5 | 70 | 67 | 450 | 1 |
| 10 | 158 | 160 | 83 | 1050 | 1 |
| 12 | 158.6 | 215 | 95 | 1410 | 1 |
| 14 | 159.3 | 230 | 100 | 1500 | 1 |

## Single line to ground fault

A single line to ground fault is simulated at PCC for the considered system operating at full load. Wind speed is assumed to be 10m/s. Simulation is repeated for different fault durations and corresponding values of the performance indices are given in Table 4. STATCOM DC link voltage Vdc is maintained at 600V before and after fault. Alternator speed and Vpcc settle at 1 pu. Fig 6 shows the plots of the parameters for a fault duration of 100ms. Table 4 shows the variations of various parameters during faults for different durations of faults. Vdc is maintained at 600V before and after fault. Alternator speed settles at 1 pu. Vpcc settles at 0.989 and 0.982pu after the fault clearance for 100ms and 625ms faults respectively.

**Table 4:** Range of transients in different parameters at SCIG terminals for single line to ground fault at PCC for a wind speed of 10m/s at full load and 0.9 power factor lagging.

| Fault duration (ms) | ω (rad/s) | P (kW) | Q (kVAR) | Te(Nm) | Vpcc(pu) | Vdc(V) |
|---|---|---|---|---|---|---|
| 100 | 157.4-160.8 | 110-210 | 76-111 | 330-1750 | 0.977-1 | 595-604 |
| 625 | 156.5-160.8 | 110-209 | 73-111 | 330-1750 | 0.97-1 | 594-605 |

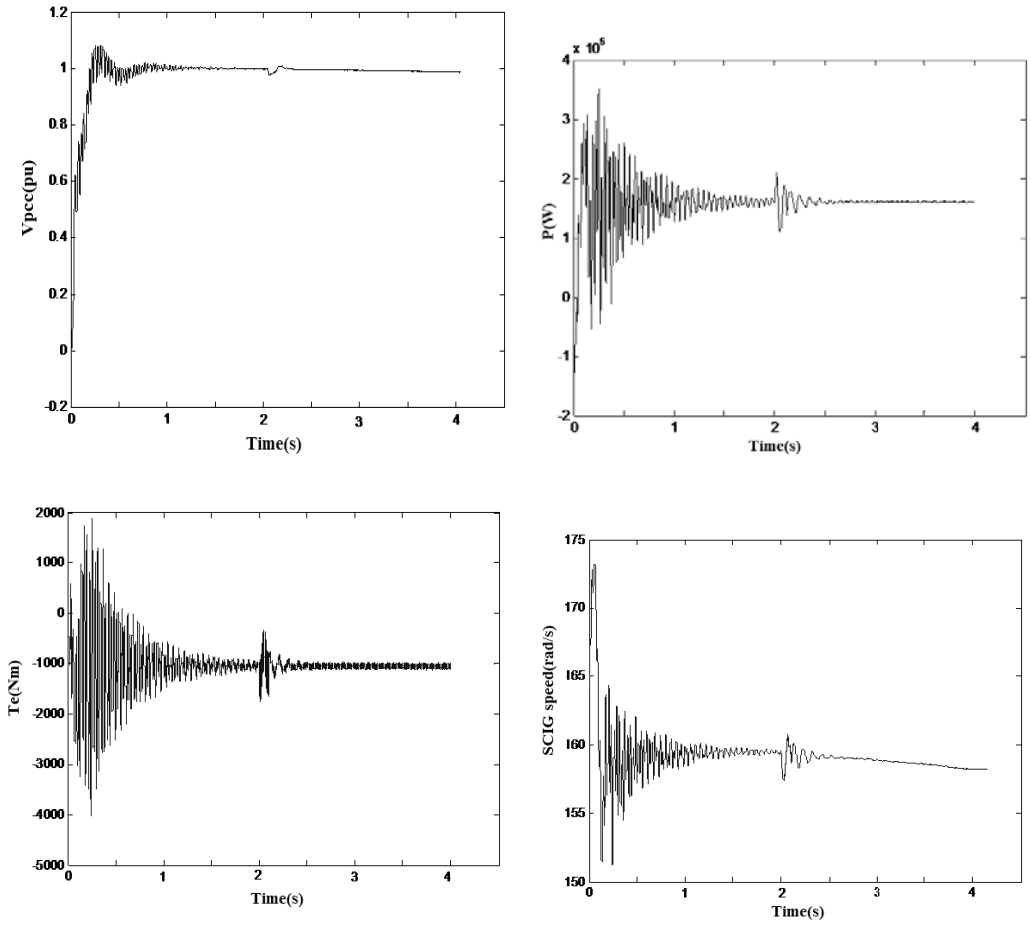


**Figure 6:** System performance indices for single line to ground fault of 100ms duration at PCC for a wind speed of 10m/s at full load of 0.9 power factor lagging

## Double line to Ground fault

A double line to ground fault is implemented at PCC. Table 5 shows the results for double line to ground fault for different durations. Fig 7 shows the variations for 100ms fault duration.

**Table 5:** Range of transients in different parameters at SCIG terminals for double line to ground fault at PCC for a wind speed of 10 m/s at full load and 0.9 power factor lagging.

| Fault duration (ms) | ω (rad/s) | P (kW) | Q (kVAR) | Te(Nm) | Vpcc(pu) | Vdc (V) |
|---|---|---|---|---|---|---|
| 100 | 152.8-170.9 | -95 to +365 | -380 to +650 | +4000 to -6280 | 0.41-1.05 | 535-625 |
| 200 | 153 -173 | -95 to +255 | -540 to +650 | +4000 to -6280 | 0.39-1.045 | 532-620 |
| 400 | 152.9-185.6 | -95 to +245 | -680 to +650 | +4000 to -6280 | 0.39-0.945 | 395-655 |

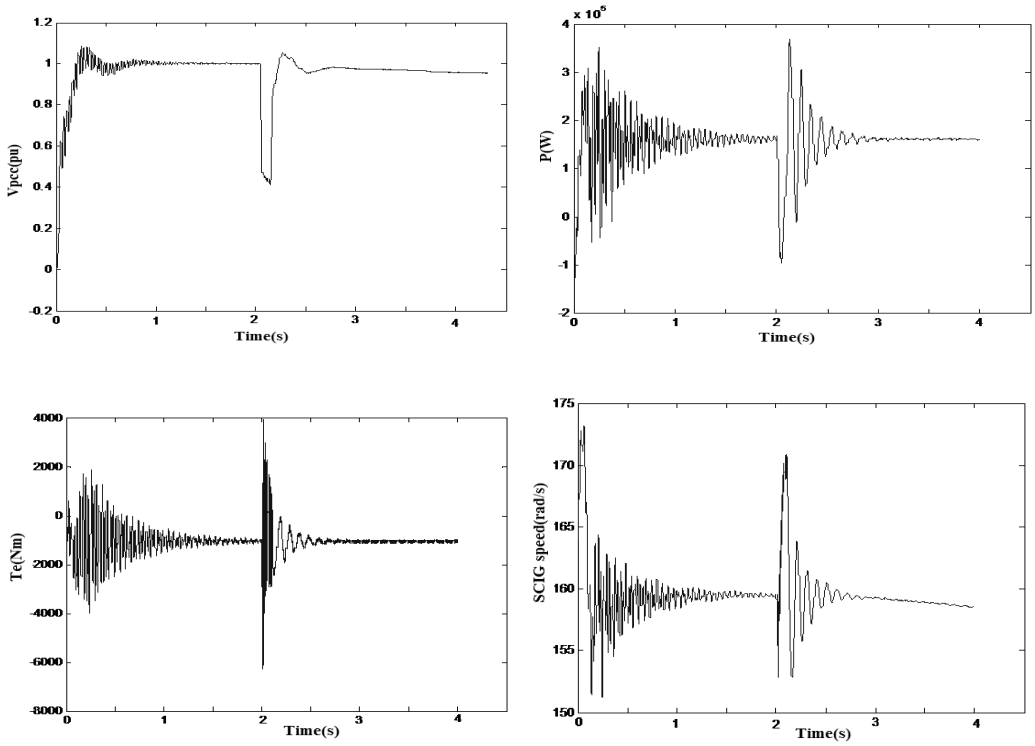


**Figure 7:** System performance indices for double line to ground fault of 100ms duration at PCC for a wind speed of 10m/s at full load of 0.9 power factor lagging

For double line faults, the alternator speed varies over the range of 0.02pu during the fault. For 100ms fault duration, Vpcc and Vdc settle at 1pu and 600V respectively. For 400ms fault duration, Vpcc and Vdc settle at respective values of 0.93 pu and 580V. When the fault duration is increased to 550ms, SCIG speed increases indefinitely and the system becomes unstable. Fig. 8(i) shows the plots for a wind speed of 10m/s at full load corresponding to 550ms fault.

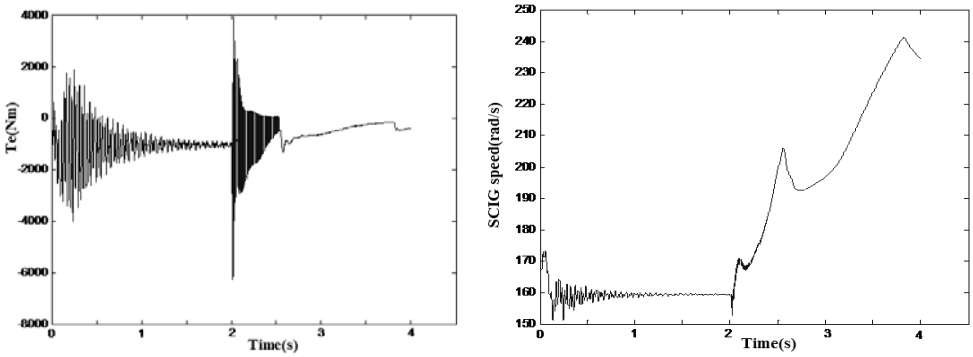


**Figure 8 (i):** System performance indices for double line to ground fault of 550ms duration at PCC for a wind speed of 10m/s at full load of 0.9 power factor lagging

When the wind speed is reduced to 8m/s from 10m/s for same type of fault and duration, the system regains to original condition and the system becomes stable. Table 6 shows the variations for 8m/s during fault conditions. Fig 8(ii) shows the plots corresponding to this condition.

**Table 6:** Range of transients in different parameters at SCIG terminals for double line to ground fault at PCC for a wind speed of 8 m/s at full load and 0.9 power factor lagging

| Fault duration (ms) | ω (rad/s) | P (kW) | Q (kVAR) | Te(Nm) | Vpcc(pu) | Vdc(V) |
|---|---|---|---|---|---|---|
| 550 | 147.4-167.5 | -150 to +142 | -440 to +660 | - 7300 to +4900 | 0.42 to 1.035 | 440-675 |

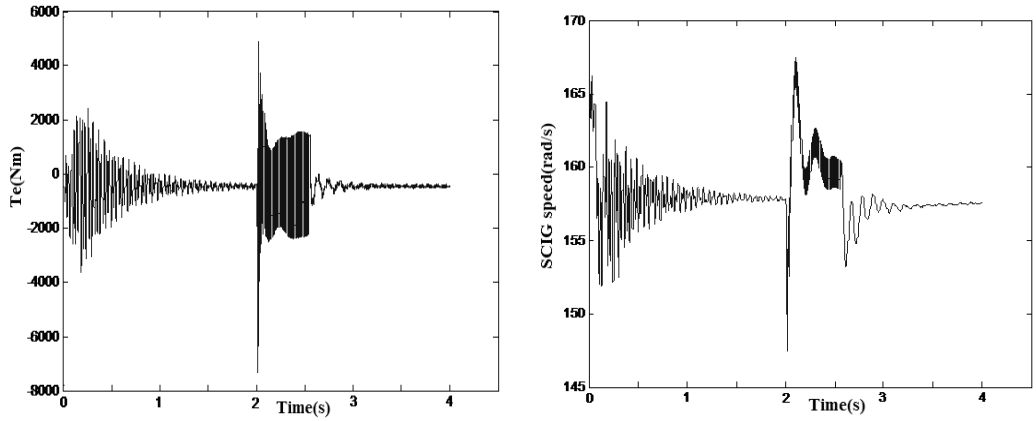


**Figure 8(ii):** System performance indices for double line to ground fault of 550ms duration at PCC for a wind speed of 8m/s at full load of 0.9 power factor lagging

For the double line fault of 550ms duration at 10m/s, the system becomes unstable. But when the load demand is reduced to half load, the system retains its stability by returning to original condition. Alternator speed settles at 1.017 pu, 7.5s after the fault clearance. SCIG speed and Te respectively settle at 171rad/s and 975Nm.Table 7 shows the parameters variations for half load.

Fig. 8(iii) show the plots of Te and SCIG speed.

**Table 7:** Range of transients in different parameters at SCIG terminals for double line to ground fault at PCC for a wind speed of 8 m/s at half load and 0.9 power factor lagging

| Fault duration (ms) | ω (rad/s) | P (kW) | Q (kVAR) | Te(Nm) | Vpcc(pu) | Vdc (V) |
|---|---|---|---|---|---|---|
| 550 | 160-182 | -150 to +255 | -540 to +640 | +5200 to -8350 | 0.41-1 | 370-660 |

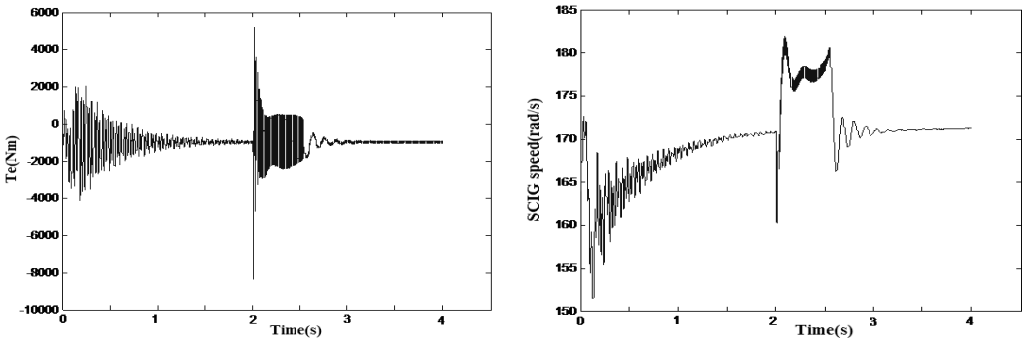


**Figure 8(iii):** System performance indices for double line to ground fault of 550ms duration at PCC for a wind speed of 10m/s at half load of 0.9 power factor lagging

## Three phase to Ground fault

A three phase to ground fault of different durations is simulated at PCC. Table 8 shows the different parameter variations and system becomes stable after the clearance of the fault. Alternator speed varies over 0.96 to 1.06pu during fault. For 50ms, 100ms and 200ms fault durations, Vpcc settle at 1pu, 0.99 pu and 0.94 pu respectively. Fig 9 shows the plots for 100ms fault. Vdc settles at 600V for 50 and 100ms fault and 580V for 200ms fault respectively.

**Table 8:** Range of transients in different parameters at SCIG terminals for three phase to ground fault at PCC for a wind speed of 10 m/s at full load and 0.9 power factor lagging

| Fault duration (ms) | ω (rad/s) | P (kW) | Q (kVAR) | Te(Nm) | Vpcc(pu) | Vdc (V) |
|---|---|---|---|---|---|---|
| 50 | 143.2-179.5 | -275 to +420 | -375 to +200 | +2670 to -8100 | 0-1.04(0.96) | 548-620 |
| 100 | 143.2-180.5 | -130 to +350 | -450 to +200 | +2675 to -8100 | 0-1.04(0.94) | 430-625 |
| 200 | 143.2-202.4 | -90 to +265 | -575 to +200 | +2700 to -8030 | 0-0.95(0.92) | 185-682 |

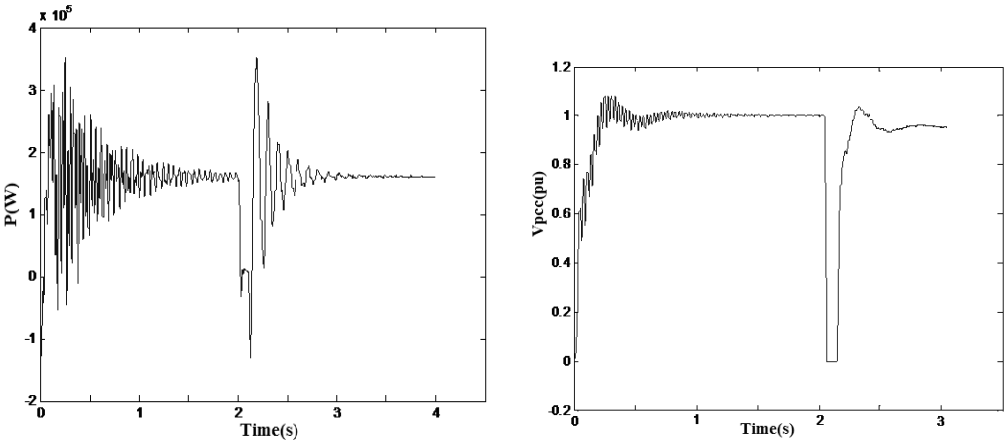

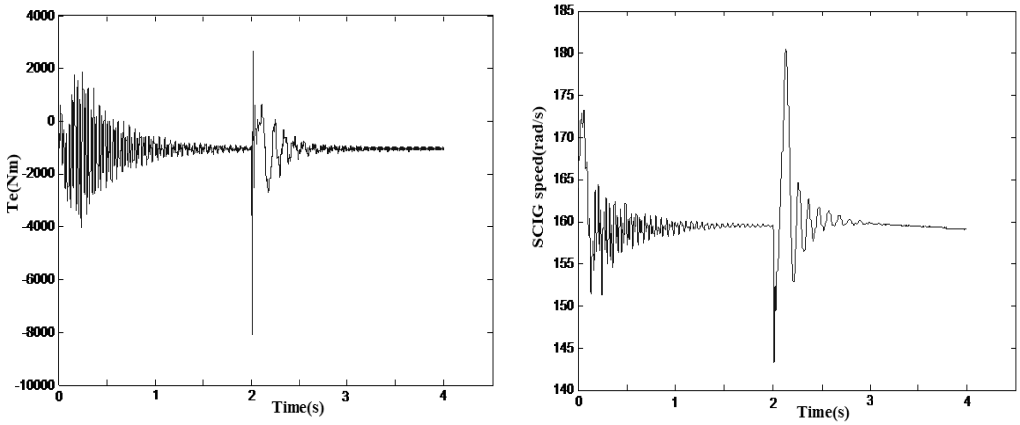


**Figure 9:** System performance indices for three phase to ground fault of 100ms duration at PCC for a wind speed of 10m/s at full load of 0.9 power factor lagging

When the fault duration is increased to 300ms, the system becomes unstable. Fig 10(i) shows the plots of Te and SCIG speed corresponding to this condition

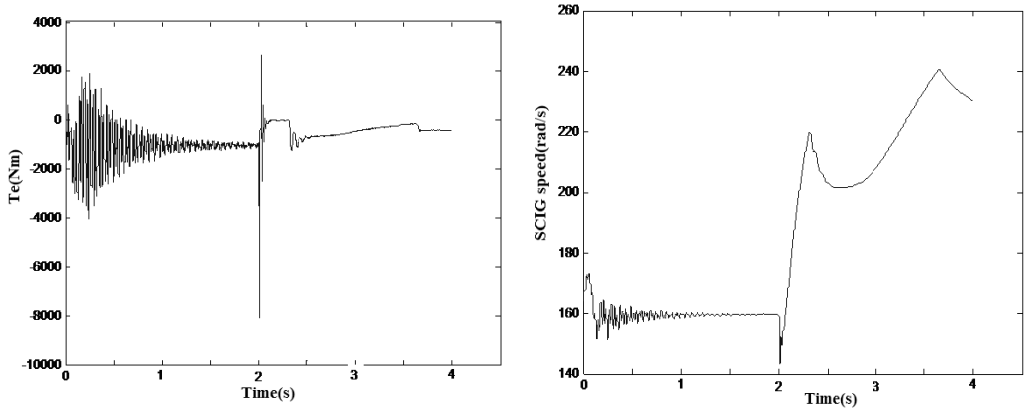


**Figure 10(i):** System performance indices for three phase to ground fault of 300ms duration at PCC for a wind speed of 10m/s at full load of 0.9 power factor lagging

For 300ms duration, the system becomes unstable for RL load of 0.9 pf lagging. If unity power factor load is used for same type and duration of fault and 10m/s wind speed, the system retains its original condition thereby stability is attained. Vpcc settles at 0.9 pu after the fault. Table 9 gives the parameter variations during fault. Fig 10(ii) shows the plots of Te and SCIG speed for this condition.

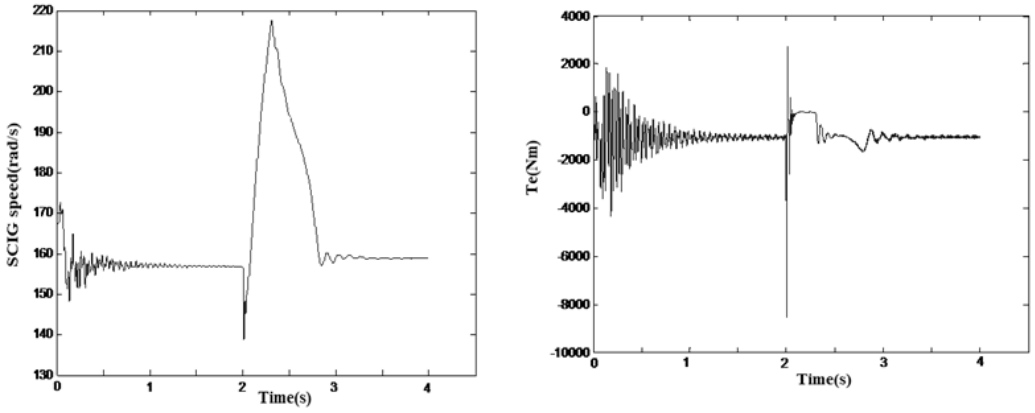


**Figure 10(ii):** System performance indices for three phase to ground fault of 300ms duration at PCC for a wind speed of 10m/s at full load of unity power factor

**Table 9:** Range of transients in different parameters at SCIG terminals for three phase to ground fault at PCC for a wind speed of 10 m/s at full load and unity power factor.

| Fault duration (ms) | ω (rad/s) | P (kW) | Q (kVAR) | Te(Nm) | Vpcc(pu) | Vdc (V) |
|---|---|---|---|---|---|---|
| 300 | 217.4-139 | -90 to +220 | -650 to +210 | +2740 to -8540 | 0-0.86 | 215-745 |

## Summary and Conclusions

(i)Table 10 gives the summary of the transient stability margin(in ms) of SCIG for a wind speed of 10m/s at different loading conditions.

**Table 10:** Transient stability margin(in ms) of SCIG for a wind speed of 10m/s at different loading conditions.

| Type of fault | Fraction of Load | | | |
|---|---|---|---|---|
| | Full load | | Half load | |
| Nature of load | RL load | R load | RL load | R load |
| Single line to ground fault | 625 | 625 | 625 | 625 |
| Double line to ground fault | 500 | 510 | 625 | 625 |
| Three phase to ground fault | 280 | 310 | 330 | 350 |

**Table 11:** Parameter variations for 150ms three phase to ground fault for STATCOM with and without supercapacitor.

| Rating | 250kVAR | 250 kVAR with supercapacitor |
|---|---|---|
| STATCOM DC link voltage Variations(V) | 130/1060 | 200/650 |
| SCIG max speed(rad/s) | 189 | 188 |
| Settling time after fault clearance (ms) | 300 | 290 |
| Recovery voltage at PCC(pu) | 0.95 | 0.96 |

(ii)Transient stability margin increases with increase in power factor of load. If the load is highly resistive, there is an improvement in transient stability margin as the load resistance offers damping effect on the speed of SCIG thereby the maximum speed is reduced. Transient stability margin of SCIG increases with decrease in load demand due to the fast dynamic performance of STATCOM.

(iii)During fault conditions, the reactive power drawn by the SCIG is very high that ordinary STATCOM is not able to supply it. When supercapacitor is used with STATCOM, large reactive power consumption is easily met making the system to come back to stable state.

(iv)From Table 11, it can be seen that, the maximum transient and dip in STATCOM DC link capacitor is reduced if supercapacitor is used with STATCOM.

(iv)During the fault the grid voltage at PCC falls because of the consumption of large reactive power drawn by SCIG and in turn the electromagnetic torque developed to match the constant mechanical torque supplied by the wind turbine declines so that the SCIG accelerates. Stability of induction machine depends on the magnitude of mechanical torque developed by wind turbine and reapplied electromagnetic torque after the fault. From Table 11, it is seen that the settling time after the fault clearance is reduced. This shows that the electromagnetic torque is developed quickly because of the fast dynamic characteristics of supercapacitor.

## References

[1] Zhengping Xi Babak Parkhideh, Subhashish Bhattacharya, ”Improving Distribution system performance with integrated STATCOM and super capacitor energy storage system”, IEEE Power Electronics Specialists Conference (PESC), 15-19 June 2008, pp.1390-1395.

[2] “Electrochemical Capacitor Characterization for Electric Utility Applications”Stanley Atcitty, Ph.D Dissertation, Virginia Polytechnic Institute and State University, USA, November 16, 2006

[3] P.Srithorn, M.Aten and R.Parashar, ”Series connection of supercapacitor modules for energy storage”, Third IET International Conference on Power Electronics, Machines and Drives, March 2006, pp. 354-360.
[4] Narain G. Hingorani, Laszlo Gyugyi, “Understanding FACTS: Concepts and Technology of Flexible AC Transmission Systems”, IEEE press, 2000.
[5] Alexey I.Belyakov, ”High voltage, high power Electrochemical supercapacitors for power quality-Technical requirements and Application peculiarities”, 16th International seminar on Double layer capacitors and Hybrid energy storage devices, 4-6 December, 2006.
[6] B.Arun Karuppaswamy, ”Synchronous reference frame strategy based STATCOM for reactive and harmonic current compensation” ’M.Tech Thesis, NIT, Calicut

## Appendix

Specifications of Wind Turbine and SCIG

**Wind Turbine**
Diameter: 28.5 m
Area of swept circle: 638 sq.m
Speed (rated) HIGH / LOW: 39.8 rpm / 26.5 rpm
Number of blades: 3
Cp max=0.44
**Gear ratio: 40**
**Generator**
Type: asynchronous
No. of poles: 4
Rated output: 250 kW
Speed: 1500 rpm
Main voltage: 400 V
Frequency: 50 Hz
**Performance Data**
Rated wind speed: 14 m/s
Cut-in wind speed: 3.5 m/s
Cut-out wind speed: 25 m/s